www.rericjournal.ait.ac.th

Energy and Exergy Analysis of Double Flow Corrugated Absorber Solar Air Heaters

Som Nath Saha[*1] and S.P. Sharma[*]

Abstract – *This paper presents the analytical investigation of the double flow flat plate and corrugated absorber solar air heaters having different configurations of flow channels. The energy balance equations are analytically derived and solved by developing a computer program in C^{++} language in order to analyze the effect of system configurations and operating parameters on energy and exergy performance. The results of different configurations of double flow corrugated absorber solar air heaters have been compared with double flow flat plate absorber solar air heater and it indicates that the corrugated absorber solar air heaters (SA-1, SA-2 and SA-3) have much higher efficiency than the flat plate solar air heater (SA-4). It is found that the maximum enhancement in energy efficiency of SA-1 solar air heater is 7.20% for the mass flow rate of 0.035 kg/s. It is also observed that the exergy efficiency become negative at higher mass flow rate (i.e. m > 0.072 kg/s) for all types of solar air heater. The results also show that increasing the solar intensity leads to achieve higher air temperature rise and efficiencies.*

Keywords – corrugated absorber, double flow, energy efficiency, exergy efficiency, solar air heater.

1. INTRODUCTION

Solar energy is one of the renewable source of energy which is convenient, sustainable, abundant and clean. Its main application is in thermal energy utilization system like solar water heater, air heater, cooker, pump, power generation etc. Among various applications of solar energy, air heating through the solar air heaters are very simple and economic. Solar air heaters are mainly used for low to medium grade thermal energy, like space heating, cooling, crop drying etc. Even though it is simple in design, low maintenance and operating cost, its efficiency is low due to poor thermophysical properties of air. To improve the performance of solar air heaters several designs are developed by many researchers. Such design includes honeycomb collectors, extended surface absorber, use of artificial roughness on the absorber plate, packing of porous material in air flow channel. One of the effective ways to improve the convective heat transfer rate is to increase the heat transfer surface area and to increase turbulence inside the channel by using fin or corrugated surfaces [1].

The energy balance method is associated with the first law of thermodynamics which is used to analyze the thermal and thermohydraulic efficiencies of an energy system. However, analysis based on the second law of thermodynamics implies reversibility or irreversibility process of an energy system. The exergy analysis involves both the first and second laws of thermodynamics, it is very important tool for design, optimization and performance evaluation of a system.

Recently, several researchers have undertaken many studies covering thermodynamic analysis of solar air heaters. Energy and exergy efficiency experimentally evaluated for a solar air heater with paraffin wax as thermal energy storage and found average energy efficiency 40.4% and exergy efficiency 4.2% [2]. Hossein *et al.* [3] developed an exergetic optimization of the solar air heater. The exergy efficiency has been compared with the thermal efficiency of air heater and found extraordinary increase in exergy efficiency according to the optimized parameters. An experimental investigation of five different air collector with staggered fins attached below the absorber plate has been conducted and present the exergy relations for all collectors and also found that the largest irreversibility occurred at conventional solar collector [4]. The energy and exergy analysis of a flat plate solar air heater with different obstacles and without obstacles have been presented and concluded that double flow collector with obstacles is better than that without obstacles [5]. By using the second law of thermodynamics, the optimum mass flow rate for maximum exergy efficiency of a flat plate collector is 0.0011 kg/s for testing conditions [6]. A comparative study has been presented for various types of artificial roughness geometries on the absorber plate of solar air heater and evaluates the performance in terms of energy, effective and exergy efficiency [7]. The first and second laws efficiency of flat plate solar air heaters have several obstacles on absorber plate and without obstacles has been investigated for two mass flow rates 0.0074 kg/s and 0.0052 kg/s and obtained the first law efficiency 20% to 82% and second law efficiency 8.32% to 44.00% [8]. Lalji, Sarviya and Bhagoria [9] developed correlations for heat transfer coefficient and friction factor for packed bed solar air heater and also they have done exergy analysis. The experiment performed on the five types of solar air heaters with porous baffles insert and compared the energy and exergy efficiencies with each other for mass flow rates of 0.016 kg/s and 0.025 kg/s. The results showed that higher efficiency for mass flow rate of 0.025 kg/s with aluminium foam of 6 mm thickness [10]. The efficiency and exergy analysis of five different

* Department of Mechanical Engineering, National Institute of Technology, Jamshedpur, Jharkhand-831014, India.

[1]Corresponding author;
Tel: +91 8582094184.
E-mail: somnath.rvs@gmail.com

types of air solar collectors have been experimentally investigated and reported that heat transfer coefficient and pressure drop increases with shape of absorber surface [11]. A packed bed solar air heater with PCM spherical capsules as packing material proposed used first and second laws of thermodynamics to obtain the energy and exergy efficiency for optimization and found energy efficiency 32% to 45% and exergy efficiency 13% to 25% [12]. The effect of depth, length, fin shape and Reynolds number studied for the energy and exergy analysis of single and two glass cover solar air collector. The study showed that the system with fin and thin metal sheet are more efficient than other systems [13]. A mathematical model has been developed to investigate the energy and exergy performance of wavy fin solar air heater for the evaluation of the effect of various complex geometries of wavy fin [14]. Exergetic performance evaluation of solar air heater with arc shaped wire rib roughened absorber plates have been investigated analytically by Mukesh and Radha [15] and found the maximum enhancement in exergetic efficiency as compared to smooth absorber solar air heater is 56% at relative roughness height (e/d) = 0.0422. The exergetic studied based on exergy loss of a double pass/glazed v-corrugated plate solar air heater and optimized exergy efficiency for different parameters of distance between two glass covers, height of v-corrugations, area of the heater and total mass flow rate [16]. Energy and exergy analysis of a flat plate solar air heater having copper tubes with extended copper fins as absorber have been investigated experimentally and found maximum energy and exergy efficiency 49.4% to 59.2% and 18.25% to 35.53%, respectively, and also observed that solar air heater with sensible heat storage have better than the conventional flat plate solar air heater without storage [17]. El-Sebaii *et al.* [18] investigated the performance of double pass flat and v-corrugated solar air heaters and found that the double pass v-corrugated have 11-14% more efficient than double pass flat plate heater. Karim and Hawlader [19] performed the effects of operating variables on the thermal performance of v-groove solar air collector for drying applications. They used flow rate range 0.01 to 0.054 kg/m^{2}s and found that v-groove collector have better thermal efficiency than a flat plate collector of similar design and suggested 0.035 kg/m^{2}s flow rate for most drying purposes. Kabeel *et al.* [20] investigated the performance of flat plate and v-corrugated plate solar air heaters with phase change material as thermal energy storage and they found that the v-corrugated plate solar air heater have better performance. A parametric study of cross corrugated solar air collectors having wavelike absorbing plate and wavelike bottom plate crosswise position performed by Wenxian *et al.* [21] and Wenfeng *et al.* [22] and found that the cross corrugated collector have superior thermal performance than that of the flat plate. Prashant and Satyender [23] analytically investigated the thermal performance of double pass flat and v-corrugated absorber plate solar air heaters under recycle operation. Based on simulation results they obtained the optimum value of the recycle ratio, the mass flow rate, the absorptivity and the emissivity at which the solar air heaters yield the maximum value of the thermal efficiency.

It is evident from the literature survey that various investigators have investigated the energy and exergy performance of flat plate, packed bed, artificial roughened, obstacles on absorber, corrugated, fins and baffles solar air heaters. In this paper two new type of solar air heaters SA-1 and SA-2 are presented as shown in Figures 1a and 1b, respectively which consist of corrugated absorber plate, bottom plate and inner glass cover, having different flow channel configurations, and entirely different from previous papers. The SA-1 solar air heater forms converging-diverging flow channels above and under the absorber plate. This configuration creates more turbulence in the flowing air in comparison to those solar air heaters having only corrugated absorber plate and enhances the heat transfer rate. The aim of present investigation is to carry out the performance evaluation based on energy and exergy of the double flow flat plate and corrugated absorber solar air heaters having different air flow configurations. The influence of performance parameters such as mass flow rate and insolation on energy, effective and exergy efficiencies have been investigated.

The main characteristics of the solar air heater considered in this study; heaters consist of double glass cover to reduce the heat losses to the surrounding, double flow in which air flows simultaneously above and under the absorbing plate in the same direction, which increases the heat transfer rate due to increase in thermal conductance. Figure 1 shows the different configuration of double flow corrugated and flat plate absorber solar air heaters. SA-1 (Figure 1a) and SA-2 (Figure 1b) have corrugated absorber plate, bottom plate and lower glass cover, having different configuration of air flow channels. SA-1 have converging-diverging air flow channel over and under the absorbing plate, which creates more turbulence in flowing air and increases the heat transfer rate. SA-3 has v-corrugated absorber with flat bottom plate and glass cover (Figure 1c). SA-4 has the flat plate absorber solar air heater (Figure 1d).

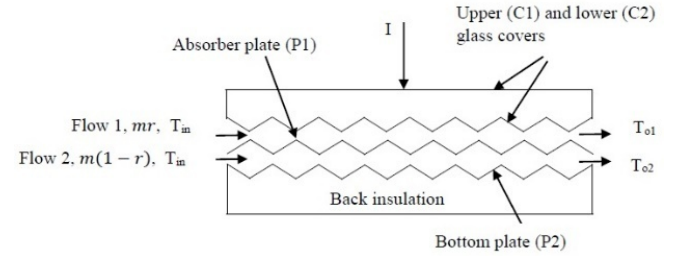

(a) SA-1

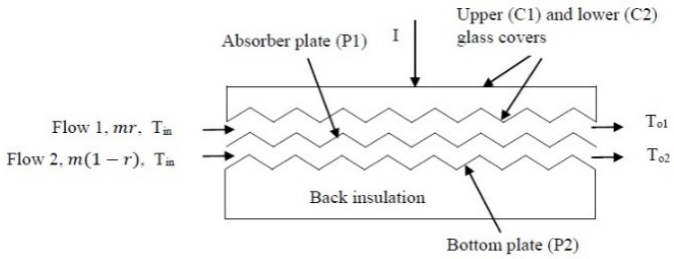

(b) SA-2

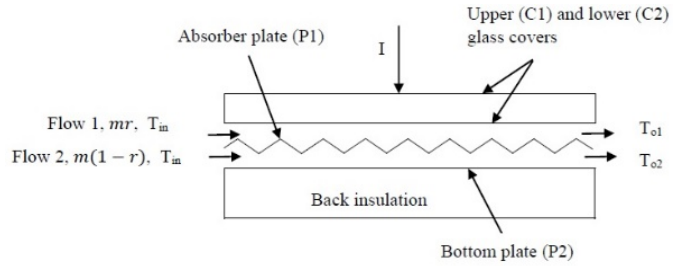

(c) SA-3

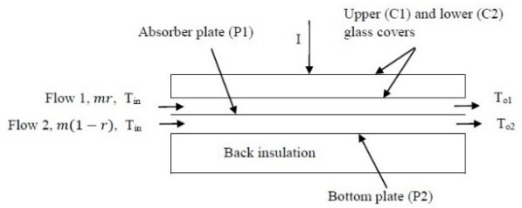

(d) SA-4

Fig. 1. Different design of double flow type solar air heaters.

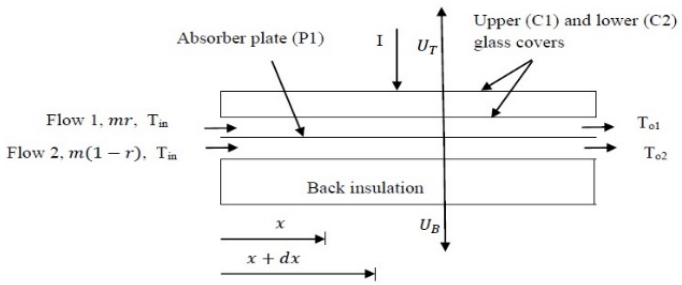

Fig. 2. The schematic diagram of double flow solar air heater.

2. THEORETICAL ANALYSIS

The schematic diagram of double flow solar air heater is shown in Figure 2. As seen in Figure 2, two air streams, above and below the absorber plate flow 1 and flow 2 respectively of different flow rates but with total flow rate remains constant. The energy balance equations have been formulated under the following assumptions [24]:

- Steady state performance of solar air heater.
- The temperatures of air varies only in the flow directions.
- There is no absorption of radiant energy by the glass covers and air streams.
- Temperature gradient does not exist along the thickness of lower and upper glass covers, absorbing plate and back plate.

- The covers are opaque to infrared radiation.
- There is no heat generation.
- Aspect ratio (W/H >> 1) is very large.

2.1. Energy Balance Equations

The energy balance equations for a differential element, dx, at a distance x for glass cover, absorber plate, bottom plate, flow 1 and flow 2 can be written as:

- Lower glass cover (C2)

$$h_{r,P1C2}(T_{P1}-T_{C2})Wdx+h_{c,F1C2}(T_{F1}-T_{C2})Wdx=U_{C2a}(T_{C2}-T_a)Wdx \quad (1)$$

- Absorber plate (P1)

$$I\alpha_{P1}\tau_{C1}\tau_{C2}Wdx=U_T(T_{P1}-T_a)Wdx+U_B(T_{P1}-\mathit{Ta}Wdx+hc,\mathrm{P1F1}\mathit{TP1}-\mathit{TF1}Wdx+hc,\mathrm{P1F2}\mathit{TP1}-\mathit{TF2}Wdx \quad (2)$$

- Bottom plate (P2)

$$h_{r,\mathrm{P1P2}}(T_{P1}-T_{P2})Wdx+h_{c,\mathrm{F2P2}}(T_{\mathrm{F2}}-T_{P2})Wdx=U_{\mathrm{P2}a}(T_{P2}-T_a)Wdx \quad (3)$$

- Air flowing over the absorber plate (F1)

$$h_{c,\mathrm{P1F1}}(T_{P1}-T_{\mathrm{F1}})Wdx=mrc_pdT_{\mathrm{F1}}+h_{c,\mathrm{F1C2}}(T_{\mathrm{F1}}-\mathit{TC2}Wdx \quad (4)$$

- Air flowing under the absorber plate (F2)

$$h_{c,\mathrm{P1F2}}(T_{P1}-T_{\mathrm{F2}})Wdx=m(1-r)c_pdT_{\mathrm{F2}}+h_{c,\mathrm{F2P2}}(T_{\mathrm{F2}}-T_{\boldsymbol{P2}})Wd \quad (5)$$

Solving Equations (1) – (3), we have:

$$T_{\boldsymbol{P1}}-T_{\mathrm{F1}}=-B_1(T_{\mathrm{F1}}-T_a)+B_2(T_{\mathrm{F2}}-T_a)+B_3 \quad (6)$$

$$T_{\mathrm{F1}}-T_{\boldsymbol{C2}}=B_4\left[\left(U_{\mathrm{C2}a}+B_1h_{r,\mathrm{P1C2}}\right)(T_{\mathrm{F1}}-T_a)-\mathit{B2}hr,\mathrm{P1C2}\mathit{TF2}-\mathit{Ta}-hr,\mathrm{P1C2}\mathit{B3} \quad (7)$$

$$T_{P1}-T_{\mathrm{F2}}=-B_5(T_{\mathrm{F2}}-T_a)+B_6(T_{\mathrm{F1}}-T_a)+B_3 \quad (8)$$

$$T_{F2}-T_{P2}=B_7\left[\left(U_{\mathrm{P2}a}+B_5h_{r,\mathrm{P1P2}}\right)(T_{\mathrm{F2}}-T_a)-\mathit{B6}hr,\mathrm{P1P2}\mathit{TF1}-\mathit{Ta}-\mathit{B3}hr,\mathrm{P1P2}$$

Substituting Equation (6) and (7) into Equation (4), yields:

$$\frac{Jrd(T_{\mathrm{F1}}-T_a)}{d\Phi}=G_1(T_{\mathrm{F1}}-T_a)+G_2(T_{\mathrm{F2}}-T_a)+G_3 \quad (10)$$

Substitution of Equation (8) and (9) into Equation (5), we have:

$$\frac{J(1-r)d(T_{\mathrm{F2}}-T_a)}{d\Phi}=G_4(T_{\mathrm{F1}}-T_a)+G_5(T_{\mathrm{F2}}-T_a)+G_6 \quad (11)$$

where, $J=\frac{mc_p}{WL}=\frac{mc_p}{A_c}$ and $\Phi=\frac{x}{L}$

The coefficients of Equations (6), (7), (8), and (9) viz B's and Equations (10) and (11) viz G's (given in Appendix A) are functions of the convective heat transfer, loss coefficients and physical properties.

Solving Equations (10) and (11) with the boundary condition:

$$\text{At, } \Phi=0, T_{\mathrm{F1}}=T_{\mathrm{F2}}=T_{\boldsymbol{F},in}$$

The temperature distributions of flow 1 and air flow 2, respectively as:

$$T_{\mathrm{F1}}=\left[\frac{A_1-\frac{G_5}{1-r}}{\frac{G_4}{(1-r)}}\right]N_1e^{\frac{A_1}{J}\Phi}+\left[\frac{A_2-\frac{G_5}{1-r}}{\frac{G_4}{(1-r)}}\right]N_2e^{\frac{A_2}{J}\Phi}-\frac{G_5}{G_4}\left(\frac{G_3G_4-G_1G_6}{G_1G_5-G_2G_4}\right)-\frac{G_6}{G_4}+T_a \quad (12)$$

$$T_{\mathrm{F2}}=N_1e^{\frac{A_1}{J}\Phi}+N_2e^{\frac{A_2}{J}\Phi}+\frac{G_3G_4-G_1G_6}{G_1G_5-G_2G_4}+T_a \quad (13)$$

The outlet temperature of flow 1 and flow 2, can be obtained from Equations (12) and (13), respectively as

$$\text{for, } \Phi=1, T_{F1}=T_{F1,o}:$$

$$T_{\mathrm{F1},o}=\left[\frac{A_1-\frac{G_5}{1-r}}{\frac{G_4}{(1-r)}}\right]N_1e^{\frac{A_1}{J}}+\left[\frac{A_2-\frac{G_5}{1-r}}{\frac{G_4}{(1-r)}}\right]N_2e^{\frac{A_2}{J}}-\frac{G_5}{G_4}\left(\frac{G_3G_4-G_1G_6}{G_1G_5-G_2G_4}\right)-\frac{G_6}{G_4}+T_a \quad (14)$$

$$\text{for, } \Phi=1, T_{F2}=T_{F2,o}$$

$$T_{F2,o}=N_1e^{\frac{A_1}{J}}+N_2e^{\frac{A_2}{J}}+\frac{G_3G_4-G_1G_6}{G_1G_5-G_2G_4}+T_a \quad (15)$$

For A_1, A_2, N_1 and N_2 referred to Appendix A.

The useful energy gain by the flow 1 and flow 2 are, respectively:

$$Q_{F1}=mrc_p\left(T_{F1,o}-T_{F,in}\right)=JrA_c\left(T_{F1,o}-T_{F,in}\right) \quad (16)$$

$$Q_{F2}=m(1-r)c_p\left(T_{F2,o}-T_{F,in}\right)=J(1-r)A_c\left(T_{F2,o}-T_{F,in}\right) \quad (17)$$

The total energy gain is

$$Q_F=Q_{F1}+Q_{F2} \quad (18)$$

The energy efficiency (η_{ene}) is:

$$\eta_{ene} = \frac{Q_F}{A_c I} = \frac{mc_p}{IA_c}\left(T_{F,o} - T_{F,in}\right) = \frac{J}{I}\Delta T \quad (19)$$

2.2 Heat Transfer Coefficients

The equation for top loss coefficient, developed by Klein [25], is used to calculate, U_T.

The bottom loss coefficient, U_B, is given by:

$$\frac{1}{U_B} = \frac{1}{U_{P2a}} + \frac{1}{h_{c,\mathrm{F2P2}}} + \frac{l_{ins}}{k_{ins}} \quad (20)$$

The thermal resistance from inner glass cover through outer glass cover to the ambient, may be expressed as:

$$\frac{1}{U_{C2a}} = \frac{1}{h_w + h_{r,C1a}} + \frac{1}{h_{c,C2C1} + h_{r,C2C1}} \quad (21)$$

where the heat transfer coefficient between two glass covers is expressed as [26]:

$$h_{c,C2C1} = 1.25\left(T_{C2,m} - T_{C1,m}\right)^{0.25} \quad (22)$$

The wind induced convective heat transfer coefficient from upper glass cover [27].

$$h_w = 5.7 + 3.8V_w \quad (23)$$

where V_w is wind speed.

By assuming mean radiant temperature equal to the mean air temperature, the radiant heat transfer coefficients between the air flow channel walls may be expressed as:

$$h_{r,P1C2} \approx \frac{4\sigma T_{F1,m}^3}{\frac{1}{\varepsilon_{P1}} + \frac{1}{\varepsilon_{C2}} - 1} \quad (24)$$

$$\text{and} \quad h_{r,P1P2} \approx \frac{4\sigma T_{F2,m}^3}{\frac{1}{\varepsilon_{P1}} + \frac{1}{\varepsilon_{P2}} - 1} \quad (25)$$

The radiant heat transfer coefficients between the two glass covers and upper glass cover to air are respectively,

$$h_{r,C2C1} = \frac{\sigma(T_{C2,m}^2 + T_{C1,m}^2)(T_{C2,m} + T_{C1,m})}{\frac{1}{\varepsilon_{C2}} + \frac{1}{\varepsilon_{C1}} - 1} \quad (26)$$

$$\text{and} \quad h_{r,C1a} = \varepsilon_{C1}\sigma(T_{C1,m}^2 + T_a^2)(T_{C1,m} + T_a) \quad (27)$$

Assuming the heat transfer coefficients between fluid and duct walls (absorbing plate and inner glass cover or bottom plate) equal,

$$h_{c,P1F1} = h_{c,F1C2} \text{ and } h_{c,P1F2} = h_{c,F2P2} \quad (28)$$

For SA-4 (flat plate absorber),

The convective heat transfer coefficient for laminar flow are calculated by using a correlation presented by Heaton *et al.* [28],

$$Nu = \frac{h_{c,P1F}D_h}{k_F} = 4.4 + \frac{0.00398(0.7ReD_h/L)^{1.66}}{1+0.0114(0.7ReD_h/L)^{1.12}} \quad (29)$$

The correlation for convective heat transfer coefficient of turbulent flow, derived from Kays [29] data with the modification of McAdams [27],

$$Nu = 0.0158Re^{0.8}[1 + (D_h/L)^{0.7}] \quad (30)$$

For SA-3 collector,

For the corrugated plate solar air heater the energy balance equations will same, the only difference is heat transfer coefficient between absorber plate to flowing fluid, because the developed surface area of the corrugated plate is increased by a factor of $1/sin(\theta/2)$ to the flat plate surface area [30] thus the heat transfer coefficient between absorber to flowing fluid is

$$h_{c,P1F} = \frac{Nuk_F}{D_h} \times \frac{1}{sin\left(\frac{\theta}{2}\right)} \quad (31)$$

The correlation of Nusselts number is presented by Karim *et al.* [30] on the basis of Hollands and Shewen [31] as:

If $Re < 2800$

$$Nu = 2.821 + 0.126\,Re\frac{2b}{L} \quad (32)$$

If $2800 \le Re \le 10^4$

$$Nu = 1.9 \times 10^{-6}Re^{1.79} + 225\frac{2b}{L} \quad (33)$$

If $10^4 \le Re \le 10^5$

$$Nu = 0.0302Re^{0.74} + 0.242Re^{0.74}\frac{2b}{L} \quad (34)$$

The correlation of Nusselts number for different collectors are present by Huseyin [11]:

For SA-2 collector,

$$Nu = 0.0437Re^{0.7728} \quad (35)$$

For SA-1 collector,

$$Nu = 0.5999Re^{0.419} \quad (36)$$

2.3 Mean Temperatures

The average (mean) air temperatures in the ducts can be expressed as:

$$T_{F1,m} = \left[\frac{A_1 - \frac{G_5}{1-r}}{\frac{G_4}{(1-r)}}\right] N_1 \frac{J}{A_1} e^{(\frac{A_1}{J}-1)} + \left[\frac{A_2 - \frac{G_5}{1-r}}{\frac{G_4}{(1-r)}}\right] N_2 \frac{J}{A_2} e^{(\frac{A_2}{J}-1)} - \frac{G_5}{G_4}\left(\frac{G_3G_4 - G_1G_6}{G_1G_5 - G_2G_4}\right) - \frac{G_6}{G_4} + T_a \quad (37)$$

$$T_{F2,m} = N_1 \frac{J}{A_1} e^{(\frac{A_1}{J}-1)} + N_2 \frac{J}{A_2} e^{(\frac{A_2}{J}-1)} + \frac{G_3G_4 - G_1G_6}{G_1G_5 - G_2G_4} + T_a \quad (38)$$

The overall loss coefficient is:

$$U_L = U_T + U_B \quad (39)$$

The average absorbing plate temperature:

$$T_{P1,m} = \frac{I\alpha_{P1}\tau_{C1}\tau_{C2} + U_L T_a + h_{c,P1F1}T_{F1,m} + h_{c,P1F2}T_{F2,m}}{U_L + h_{c,P1F1} + h_{c,P1F2}} \quad (40)$$

The average temperature of lower glass cover

$$T_{C2,m} = \frac{U_{C2a}T_a + h_{r,P1C2}T_{P1,m} + h_{c,F1C2}T_{F1,m}}{U_{C2a} + h_{r,P1C2} + h_{c,F1C2}} \quad (41)$$

The average temperature of upper glass cover

$$T_{C1,m} = \frac{(h_{c,C2C1} + h_{r,C2C1})T_{C2,m} + h_{c,C1a}T_a}{h_{c,C2C1} + h_{r,C2C1} + h_{c,C1a}} \quad (42)$$

2.4 Effective Energy Efficiency

This net energy gain (Q_{ne}) can be written as:

$$Q_{ne} = Q_F - P_m/C_f \quad (43)$$

where $P_m = m\Delta P/\rho$ is the work energy lost in friction in the heater channel, C_f is the conversion factor and is taken 0.2 [13]. Total pressure drop ΔP expressed as:

$$\Delta P = \Delta P_{ch} + \Delta P_{en} + \Delta P_{ex} \quad (44)$$

The channel pressure drop can be calculated as [18];

$$\Delta P_{ch} = 2\rho v_{ch}^2 f L/D_h \quad (45)$$

The correlations of friction coefficient for turbulent flow [11]:

For SA-4 collector,

$$f = 0.4053Re^{-0.8851} \quad (46)$$

For SA-2 collector,

$$f = 0.9564Re^{-0.743} \quad (47)$$

For SA-1 collector,

$$f = 1.0866Re^{-0.6635} \quad (48)$$

The entrance and exit pressure drop calculated as [32];

$$\Delta P_{en} + \Delta P_{ex} = (Rf_{en} + Rf_{ex})\frac{\rho v_p^2}{2} \quad (49)$$

The sum of entrance and exit resistance factor ($Rf_{en} + Rf_{ex}$) is taken as 1.5 [33].

The effective energy efficiency of the solar air heater can be expressed as;

$$\eta_{eff} = \frac{Q_{ne}}{A_c I} = \frac{Q_F - (P_m/C_f)}{A_c I} \quad (50)$$

2.5 Exergy Efficiency

The exergy balance equation can be written as [8],

$$\sum Ex_{in} - \sum Ex_o = \sum Ex_{dest} \quad (51)$$

$$\text{or } Ex_{ht} - Ex_w + Ex_{in} - Ex_o = Ex_{dest} \quad (52)$$

The general rate form of the exergy balance equation can also be expressed as:

$$\sum\left(1 - \frac{T_e}{T_s}\right)Q_s - \dot{W} + \sum m_{in}\varphi_{in} - \sum m_o\varphi_o = Ex_{dest} \quad (53)$$

$$\text{where } \varphi_{in} = (h_{in} - h_e) - T_e(s_{in} - s_e) \quad (54)$$

$$\varphi_o = (h_o - h_e) - T_e(s_o - s_e) \quad (55)$$

Substituting Equations (54) and (55) in Equation (53), it can written as:

$$\left(1 - \frac{T_e}{T_s}\right)Q_s - m[(h_o - h_{in}) - T_e(s_o - s_{in})] = Ex_{dest} \quad (56)$$

$$\text{where } Q_s = I\alpha_{P1}\tau_{C1}\tau_{C2}A_c \quad (57)$$

The change in enthalpy and entropy of air is expressed as:

$$\Delta h = h_o - h_{in} = C_p(T_{F,o} - T_{F,in}) \quad (58)$$

$$\Delta s = s_o - s_{in} = C_p ln\frac{T_{F,o}}{T_{F,in}} - Rln\frac{P_o}{P_{in}} \quad (59)$$

Substituting Equations (58) and (59) in Equation (56), it can be written as:

$$\left(1 - \frac{T_e}{T_s}\right)I\alpha_{P1}\tau_{C1}\tau_{C2}A_c - mC_p(T_{F,o} - T_{F,in}) + mC_pT_e ln\frac{T_{F,o}}{T_{F,in}} - mRT_e ln\frac{P_o}{P_{in}} = Ex_{dest} \quad (60)$$

The exergy destruction or the irreversibility can be expressed as:

$$Ex_{dest} = T_e S_{gen} \quad (61)$$

The exergy efficiency is calculated as:

$$\eta_{exe} = \frac{Ex_o}{Ex_{in}} = \frac{m(\Delta h - T_e \Delta s)}{\left(1 - \frac{T_e}{T_s}\right) Q_s} \quad (62)$$

2.6 Calculation Procedure for Energy, Effective and Exergy Efficiencies

For the numerical calculation of energy, effective and exergy efficiencies a program in C^{++} language have been developed considering the following system and operating parameters:

$L = 1.25\,m$, $W = 0.80\,m$, $H_C = 0.025\,m$, $H_{min} = 0.02\,m$, $H_{max} = 0.045m$, $\tau_{C1} = \tau_{C2} = 0.875$, $\alpha_{P1} = 0.96$, $\varepsilon_{C1} = \varepsilon_{C2} = 0.94$, $\varepsilon_{P1} = 0.80$, $\varepsilon_{P2} = 0.94$, $U_B \approx 0$, $T_a = 30℃ = 303K$, $V = 1\,m/s$, $b = 0.00625\,m$, $I = 200 - 1000\,W/m^2$, $m = 0.035 - 0.083\,kg/s$, r = 0.5.

The procedure for calculation of energy, effective and exergy efficiencies are, first using guess temperature the heat transfer coefficients have been calculated from Equations (22) to (36) then new temperatures are obtained by using Equations (37) to (42). If the calculated values of temperature are different from the assumed values continued calculation by iteration method. These new temperatures will be then used as the guess temperatures for next iteration and the process will be repeated until all the difference between newest temperatures and their respective previous values were less than 0.001. Using Equation (19), energy efficiency is calculated. Further pressure drop has been estimated using Equation (44). Then effective efficiency has been calculated by using Equation (50). The changes in enthalpy and entropy have been calculated using Equations (58) and (59), respectively, then exergy efficiency was calculate using Equation (62).

3. MODEL VALIDATION

The numerically calculated energy efficiency of different solar air heaters have been compared with the experimental values obtained from [18]. Figure 3 shows the comparison of analytical results of present work with experimental values of energy efficiency [18] of double flow flat plate (SA-4) and corrugated absorber (SA-3) solar air heater. The maximum deviation of theoretical values of energy efficiency for flat plate collector (SA-4) is found to be 2.42% and for corrugated collector (SA-3) it is 2.52%. Figure also shows the comparison of energy efficiency of various types of corrugated collectors with flat plate collector for the same parameters and found there is considerable enhancement in energy efficiency for SA-1 and SA-2 collectors. The efficiency enhancement for SA-1 collector is found to be 21.00% and 15.96% at the mass flow rate of 0.04 kg/s and 0.06 kg/s, respectively with respect to flat plate collector (SA-4). This shows good resemblance of theoretical and experimental values which makes validation of calculated numerical data with mathematical modeling.

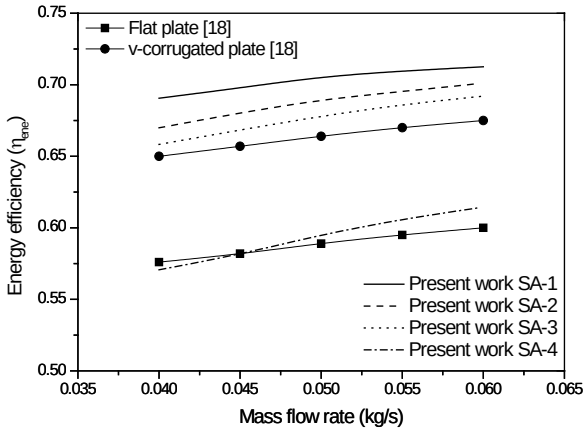

Fig. 3. Comparison of analytical energy efficiency data with available experimental data.

4. RESULTS AND DISCUSSION

In this section, the effect of mass flow rate and insolation on air temperature rise, energy, effective and exergy efficiencies are presented for various system and operating parameters.

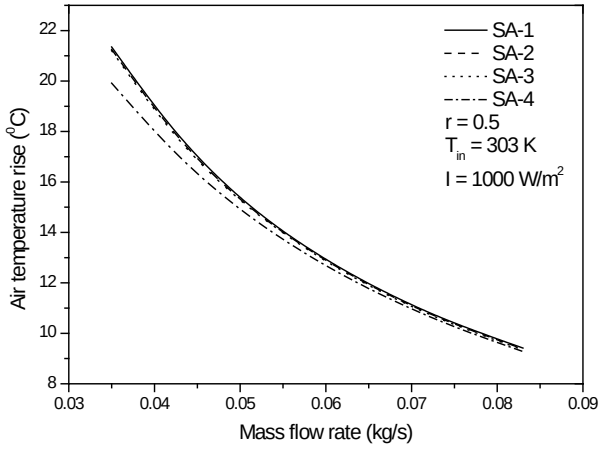

Fig. 4. Variation of air temperature rise with mass flow rate.

Figure 4 shows the variation of air temperature rise for double flow flat and corrugated absorber solar air heaters with mass flow rate for I = 1000 W/m^2. Air temperature rise continuously decreases with increase in mass flow rate for all types of solar air heaters. It is seen from the figure that the considerable amount of gain in air temperature rise at lower mass flow rate is observed due to corrugated absorber however at higher mass flow rate gain in air temperature rise is almost equal for all collectors. The maximum value of air temperature rise is 21.35°C for SA-1 collector at m = 0.035 kg/s.

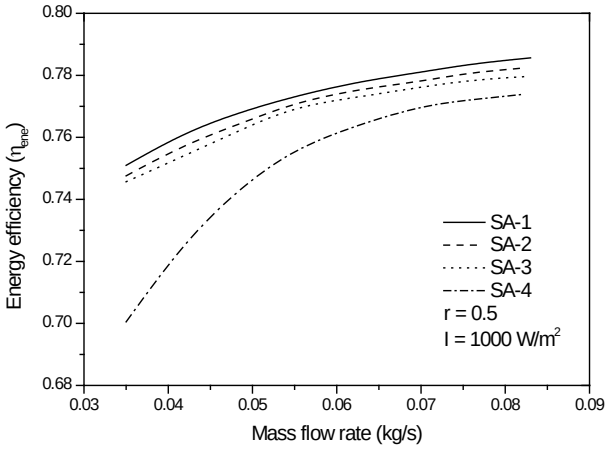

Fig. 5. Variation of energy efficiency with mass flow rate.

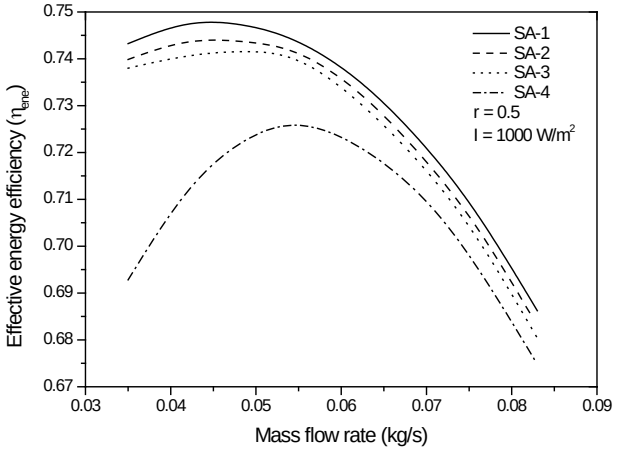

Fig. 6. Variation of effective energy efficiency with mass flow rate.

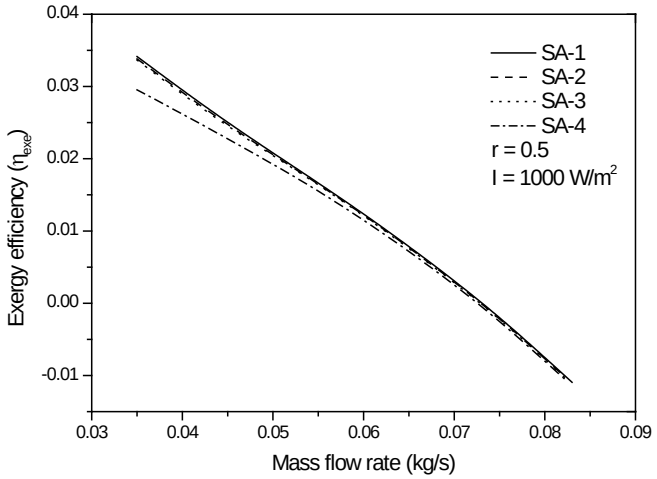

Fig. 7. Variation of exergy efficiency with mass flow rate.

Figure 5 illustrate the effect of mass flow rate on energy efficiency for a set of parameters. Energy efficiency increases with increase in mass flow rate due to increase in thermal conductance from absorber to flowing air. It can be observed that at lower mass flow rate, percentage enhancement in efficiency of corrugated absorber to flat plate collector is higher and at higher mass flow rate it is low. The SA-1 collector has the maximum energy efficiency throughout the mass flow rate investigated. The percentage enhancement in efficiency of SA-1 collector with respect to SA-4 collector is 7.20% and 1.50% at m = 0.035 kg/s and 0.83 kg/s, respectively.

Figure 6 shows the variation of effective energy efficiency with mass flow rate of air for corrugated and flat plate solar air heaters for I = 1000 W/m^2. From the figure it is seen that effective energy efficiency increases up to a certain value of mass flow rate at which it attains a maximum value and there after decreases sharply. It is also observed that the effective energy efficiency of double flow flat plate solar air heater reaches maximum value at m = 0.055 kg/s whereas for other collectors (SA-3, SA-2 and SA-1) the pick values of effective energy efficiency shifted towards lower mass flow rates of 0.050 kg/s, 0.046 kg/s and 0.044 kg/s, respectively. This type of trends is observed due to increase in pressure drop of flowing air in case of corrugated absorber / channels. The SA-1 attains the maximum value of effective energy efficiency 74.8% at m = 0.044 kg/s.

Figure 7 present the effect of mass flow rate on exergy efficiency for double flow corrugated and flat plate solar air heaters at I = 1000 W/m^2. The exergy efficiency decreases with increase in mass flow rate and it's negative at higher mass flow rate (*i.e.* m > 0.072 kg/s for all collectors). It can be observed that double flow corrugated plate leads to exergy efficiency increase compared to flat plate solar air heater. It is also observed from the figure that corrugated plate collector is more efficient at lower mass flow rate and enhancement in exergy efficiency decreases with increase in mass flow rate, due to decrease in outlet temperature of air at higher mass flow rate.

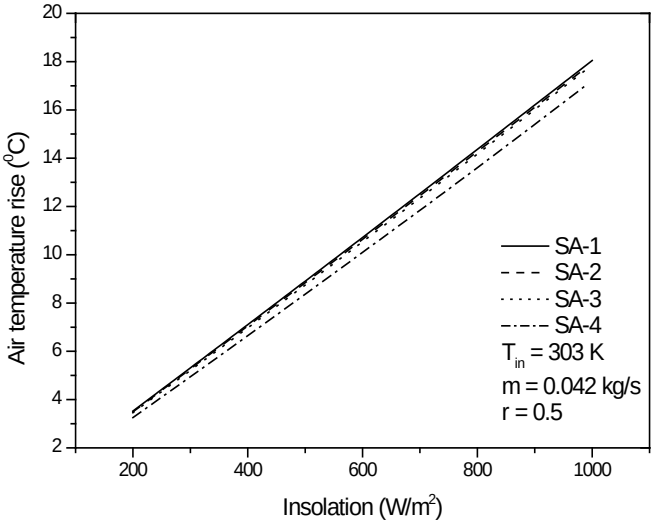

Fig. 8. Variation of air temperature rise with insolation.

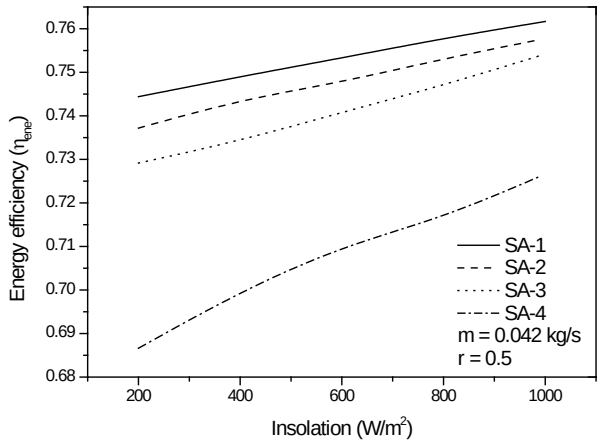

Fig. 9. Variation of energy efficiency with insolation.

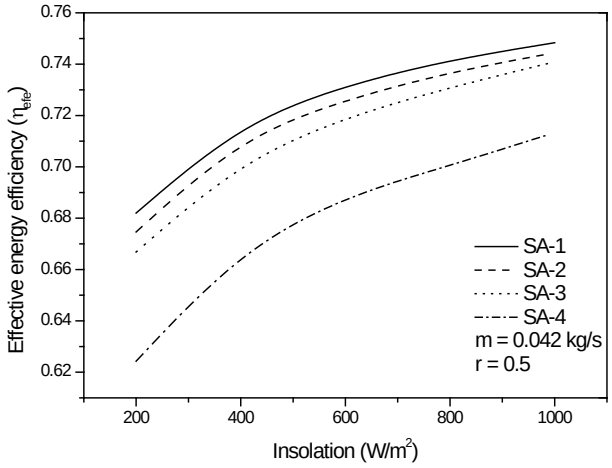

Fig. 10. Variation of effective energy efficiency with insolation.

The variation of air temperature rise with insolation, for flat plate and corrugated absorber collectors at m = 0.042 kg/s, are shown in Figure 8. It evident that air temperature rise increase linearly with increase in insolation. It is also evident from the figure that corrugated absorber collectors have higher air temperature rise to the flat plate collector. The maximum air temperature rise is 18.0°C at I = 1000 W/m^2 for SA-1 collector.

Figure 9 present the variation of energy efficiency as a function of insolation at m= 0.042kg/s for the range of insolation 200 – 1000 W/m^2. It is observed from the figure, energy efficiency increases with increase in insolation even so, percentage enhancement of efficiency decrease with increase in insolation. This is probably because of increase in insolation, increases the thermal radiation heat losses from the absorbing plate to bottom plate and to the glass cover but monotonically reduced the thermal radiation heat loss from the glass cover to the sky.

Figure 10 shows the effect of insolation on effective energy efficiency for m = 0.042 kg/s. It can be observed that effective energy efficiency monotonically increases with increase in insolation then a slight fall is observed in the rate of increase of effective energy efficiency as insolation increases due to at lower insolation heat losses to the surrounding is low and at high insolation heat losses to the surrounding is high. The corrugated collectors have much higher effective energy efficiencies than the flat plate collector (SA-4) and SA-1 collector performs superior to the SA-2 and SA-3 collector for all the values of insolation considered. This is because of increase in turbulence of air flow leads to increase convective heat transfer rate.

The variation of exergy efficiency with insolation for different solar air heaters are shown in Figure 11. As seen from the figure exergy efficiency continuously increases with increase in insolation for the mass flow rate of 0.042 kg/s. At higher insolation the exergy efficiency is high because of exergy efficiency is the function of outlet temperature of air. The outlet temperature of air is high at higher insolation. It is also seen that for lower insolation (*i.e.* I < 350 W/m^2) exergy efficiency become negative for all collectors. This type of trend is observed due to outlet temperature of air is low at lower insolation.

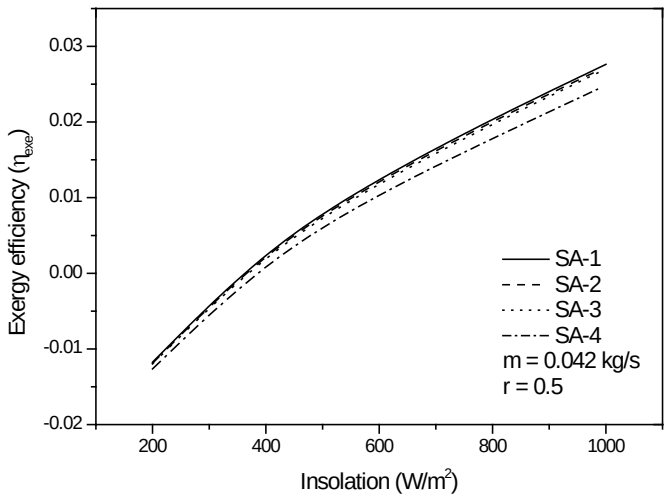

Fig. 11. Variation of exergy efficiency with insolation.

5. CONCLUSIONS

On the basis of above results the following conclusions are drawn:

i) The mathematical model for double flow solar air heater have been developed to study the effect of mass flow rate and insolation on the energy, effective and exergy efficiencies of collector.

ii) For solving the mathematical model a computer program in C^{++} language has been developed and obtained the numerical solutions.

iii) The maximum deviation between the theoretical and experimental values of energy efficiency are found to be 2.42 % and 2.52 % for SA-4 and SA-3 collectors, respectively.

iv) It is observed that energy efficiency increases while the air temperature rise decreases with increase in mass flow rate however, effective energy efficiency increases upto a certain limiting value of mass flow rate and then there after decreases sharply.

v) It is also observed that at lower mass flow rate, percentage enhancement in energy efficiency of corrugated absorber to flat plate collector is higher and at higher mass flow rate is low, the percentage enhancement in energy efficiency of SA-1 collector with respect to SA-4 collector is 7.20% and 1.50% at m = 0.035 kg/s and 0.83 kg/s, respectively.

vi) It has been found that the effective energy efficiency of double flow flat plate solar air heater reaches maximum value at m = 0.055 kg/s whereas for other collectors (SA-3, SA-2 and SA-1) the pick values of effective energy efficiency shifted towards lower mass flow rates of 0.050 kg/s, 0.046 kg/s and 0.044 kg/s, respectively.

vii) The exergy efficiency decreases with increase in mass flow rate, because of at higher mass flow rate the outlet temperature of air is low. At higher mass flow rate *i.e.* m > 0.072 kg/s the exergy efficiency become negative.

viii) For a specific mass flow rate; air temperature rise, energy, effective and exergy efficiency increases with increase in insolation for all type of collectors.

ix) It has been found that the percentage enhancement of energy efficiency and increasing rate of effective energy efficiency decrease with increase in insolation.

x) For mass flow rate of 0.042 kg/s, the exergy efficiency become negative for lower values of insolation *i.e.* I < 350 W/m^2 for all collectors.

NOMENCLATURE

A_c	Area of collector (m^2)
b	Half height of v-groove (m)
C_p	Specific heat of air at constant pressure (J/kgK)
D_h	Hydraulic diameter (m)
Ex	Exergy (W)
f	Friction coefficient
H	Height of air flow channel (m)
H_C	Height of glass cover (m)
h_c	Convective heat transfer coefficient (W/m^2 K)
h_r	Radiative heat transfer coefficient (W/m^2 K)
h	Specific enthalpy (J/kg)
I	Insolation (W/m^2)
k	Thermal conductivity (W/m K)
L	Collector length (m)
l	Thickness (m)
m	Mass flow rate (kg/s)
Nu	Nusselt number
P	Fluid pressure (N/m^2)
Q	Energy gain by air (W)
R	Universal gas constant (J/kg K)

Re Reynolds number

Rf Resistance factor

r Fraction of mass flow rate

s Specific entropy (J/kg K)

T Temperature (K)

U Loss coefficient (W/m^2 K)

V_w Velocity of wind (m/s)

v Velocity of air (m/s)

W Collector width (m)

$\dot{W}$ Work rate or power (W)

Greek symbols

α Absorptivity

ε Emissivity

ΔP Pressure drop (N/m^2)

η Efficiency

ρ Density of air (kg/m^3)

σ Stefan-Boltzmann constant (W/m^2 K^4)

τ Transmissivity

θ Angle of v-groove absorbing plate (60˚)

φ Specific exergy (J/kg)

Subscripts

a Ambient

B Bottom

F Flow

$F1$ Flow above the absorber plate

$F2$ Flow under the absorber plate

$P1$ Absorber plate

$P2$ Bottom plate

ch Channel

$dest$ Destruction

e Environment

efe Effective energy

en Entrance

ene Energy

ex Exit

exe Exergy

C Glass cover

$C1$ Upper glass cover

$C2$ Lower glass cover

ht Heat

in Inlet

ins Insulation

L Overall

m Mean

max Maximum

min Minimum

ne Net energy

o Outlet

p Pipe

s Sun

T Top

w Work

REFERENCES

[1] Goldstein L. and E.M. Sparrow. 1976. Experiments on the transfer characteristics of a corrugated fin and tube heat exchanger configuration. *Transaction of the ASME, Journal of Heat Transfer* 98: 26-34.

[2] Ozturk H.H., 2005. Experimental evaluation of energy and exergy efficiency of a seasonal latent heat storage system for greenhouse heating. *Energy Conversion and Management* 46: 1523-1542.

[3] Ajam H., Farahat S. and Sarhaddi F., 2005. Exergetic optimization of solar air heaters and comparison with energy analysis. *International Journal of Thermodynamics* 8(4): 183-190.

[4] Ucar A. and M. Inalli. 2006. Thermal and exergy analysis of solar air collectors with passive augmentation techniques. *International Communications in Heat and Mass Transfer* 33: 1281-1290.

[5] Esen H., 2008. Experimental energy and exergy analysis of a double-flow solar air heater having different obstacles on absorber plates. *Building and Environment* 43:1046-1054.

[6] Mohseni L.E., Taherian H., Masoodi R. and Reisel J.R., 2009. An energy and exergy study of a solar thermal air collector. *Thermal Science* 13(1):205-216.

[7] Gupta M.K. and S.C. Kaushik. 2009. Performance evaluation of solar air heater for various artificial roughness geometries based on energy, effective and exergy efficiencies. *Renewable Energy* 34:465-476.

[8] Kavak E., Akpinar and Kocyigit F., 2010. Energy and exergy analysis of a new flat-plate solar air heater having different obstacles on absorber plates. *Applied Energy* 87: 3438-3450.

[9] Lalji M.K., Sarviya R.M. and Bhagoria J.L., 2012. Exergy evaluation of packed bed solar air heater. *Renewable and Sustainable Energy Reviews* 16: 6262-6267.

[10] Bayrak F., Oztop H.F. and Hepbasli A., 2013. Energy and exergy analyses of porous baffles

inserted solar air heaters for building applications. *Energy and Buildings* 57: 338-345.

[11] Benli H., 2013. Experimentally derived efficiency and exergy analysis of a new solar air heater having different surface shapes. *Renewable Energy* 50:58-67.

[12] Bouadila S., Lazaar M., Skouri S., Kooli S. and Farhat A., 2014. Energy and exergy analysis of a new solar air heater with latent storage energy. *International Journal of Hydrogen Energy* 39(27): 15266-15274.

[13] Bahrehmand D., Ameri M. and Gholampour M., 2015. Energy and exergy analysis of different solar air collector systems with forced convection. *Renewable Energy* 83:1119-1130.

[14] Priyam A., Chand P. and Sharma S.P., 2016. Energy and exergy analysis of wavy finned absorber solar air heater. *International Energy Journal* 16: 119-130.

[15] Sahu M.K. and R.K. Prasad, 2016. Exergy based performance evaluation of solar air heater with arc-shaped wire roughened absorber plate. *Renewable Energy* 96: 233-243.

[16] Hedayatizadeh M., Sarhaddi F., Safavinejad A., Ranjbar F. and Chaji H., 2016. Exergy loss-based efficiency optimization of a double-pass/glazed v-corrugated plate solar air heater. *Energy* 94: 799-810.

[17] Kalaiarasi G., Velraj R. and Swami M.V., 2016. Experimental energy and exergy analysis of a flat solar air heater with a new design of integrated sensible heat storage. *Energy* 111: 609-619.

[18] El-Sebaii A.A., Aboul-Enein S., Ramadan M.R.I., Shalaby S.M. and Moharram B.M., 2011. Investigation of thermal performance of double pass flat and v-corrugated plate solar air heaters. *Energy* 36: 1076-1086.

[19] Azharul K.M. and M.N.A. Hawlader. 2006. Performance evaluation of a v-groove solar air collector for drying applications. *Applied Thermal Engineering* 26: 121-130.

[20] Kabeel A.E., Khalil A., Shalaby S.M. and Zayed M.E., 2016. Experimental investigation of thermal performance of flat and v-corrugated plate solar air heaters with and without PCM as thermal energy storage. *Energy Conversion and Management* 113: 264-272.

[21] Lin W., Gao W. and Liu T., 2006. A parametric study on the thermal performance of cross corrugated solar air collectors. *Applied Thermal Engineering* 26: 1043-53.

[22] Gao W., Lin W., Liu T. and Xia C., 2007. Analytical and experimental studies on the thermal performance of cross corrugated and flat pate solar air heaters. *Applied Energy* 84: 425-441.

[23] Dhiman P. and S. Singh, 2015. Thermal performance assessment of recyclic double-pass flat and v-corrugated plate solar air heaters. *International Journal of Sustainable Energy*: 1-23.

[24] Duffie J.A. and W.A. Backman. 1980. *Solar Engineering of Thermal Processes*. New York: Wiley.

[25] Klein S.A., 1975. Calculation of flat plate loss coefficients. *Solar Energy* 17: 79-80.

[26] Hottel H.C. and B.B. Woertz. 1942. Performance of flat plate solar heat collectors. *Transactions of the ASME* 64: 91-104.

[27] McAdams W.H., 1954. *Heat Transmission.* New York: McGraw-Hill.

[28] Heaton H.S., Reynolds W.C. and Kays W.M., 1964. Heat transfer in annular passages simultaneous development of velocity and temperature fields in laminar flow. *International Journal of Heat Mass Transfer* 7: 763-781.

[29] Kays W.M., 1980. *Convective Heat and Mass Transfer*. New York: McGraw Hill.

[30] Karim M.A., Perez E. and Amin Z.M., 2014. Mathematical modelling of counter flow v-grove solar air collector. *Renewable Energy* 67: 192-201.

[31] Hollands K.G.T. and E.C. Shewen. 1981. Optimization of flow passage geometry for air heating plate type solar collectors. *ASME Journal Solar Energy Engineering* 103: 323-330.

[32] Hegazy A.A., 2000. Thermohydraulic performance of air heating solar collectors with variable width, flat absorber plates. *Energy Conversion Management* 41: 1361-1378.

[33] Griggs E.I. and F.K. Sharifabad. 1992. Flow characteristics in rectangular ducts. *ASHRAE Transactions* 98(1): 116-127.

APPENDIX A

$$B_1 = \frac{U_T + U_B + h_{c,\mathrm{P1F2}}}{U_T + U_B + h_{c,\mathrm{P1F1}} + h_{c,\mathrm{P1F2}}} \quad \text{(i)}$$

$$B_2 = \frac{h_{c,\mathrm{P1F2}}}{U_T + U_B + h_{c,P1F1} + h_{c,\mathrm{P1F2}}} \quad \text{(ii)}$$

$$B_3 = \frac{I\alpha_{P1}\tau_{C1}\tau_{C2}}{U_T + U_B + h_{c,\mathrm{P1F1}} + h_{c,\mathrm{P1F2}}} \quad \text{(iii)}$$

$$B_4 = \frac{1}{h_{r,\mathrm{P1C2}} + h_{c,\mathrm{F1C2}} + U_{\mathrm{C2}a}} \quad \text{(iv)}$$

$$B_5 = \frac{U_T + U_B + h_{c,\mathrm{P1F1}}}{U_T + U_B + h_{c,\mathrm{P1F1}} + h_{c,\mathrm{P1F2}}} \quad \text{(v)}$$

$$B_6 = \frac{h_{c,P1F1}}{U_T + U_B + h_{c,\mathrm{P1F1}} + h_{c,\mathrm{P1F2}}} \quad \text{(vi)}$$

$$B_7 = \frac{1}{h_{r,\mathrm{P1P2}} + h_{c,\mathrm{F2P2}} + U_{\mathrm{P2}a}} \quad \text{(vii)}$$

$$G_1 = -B_1 h_{c,\mathrm{P1F1}} - B_4 h_{c,\mathrm{F1C2}} U_{C2a} - B_1 B_4 h_{c,\mathrm{F1C2}} h_{r,\mathrm{P1C2}} \quad \text{(viii)}$$

$$G_2 = B_2 h_{c,\mathrm{P1F1}} + B_2 B_4 h_{c,\mathrm{F1C2}} h_{r,\mathrm{P1C2}} \quad \text{(ix)}$$

$$G_3 = B_3 h_{c,\mathrm{P1F1}} + B_3 B_4 h_{c,F\mathrm{1C2}} h_{r,\mathrm{P1C2}} \quad \text{(x)}$$

$$G_4 = B_6 h_{c,\mathrm{P1F2}} + B_6 B_7 h_{c,\mathrm{F2P2}} h_{r,\mathrm{P1P2}} \quad \text{(xi)}$$

$$G_5 = -B_5 h_{c,\mathrm{P1F2}} - B_7 h_{c,\mathrm{F2P2}} U_{\mathrm{P2}a} - B_5 B_7 h_{c,\mathrm{F2P2}} h_{r,\mathrm{P1P2}} \quad \text{(xii)}$$

$$G_6 = B_3 h_{c,\mathrm{P1F2}} + B_3 B_7 h_{c,\mathrm{F2P2}} h_{r,\mathrm{P1P2}} \quad \text{(xiii)}$$

$$A_1 = \frac{1}{2}\left[\left(\frac{G_1}{r} + \frac{G_5}{(1-r)}\right) + \sqrt{\left(\frac{G_1}{r} - \frac{G_5}{(1-r)}\right)^2 + \frac{4G_2G_4}{r(1-r)}}\right] \quad \text{(xiv)}$$

$$A_2 = \frac{1}{2}\left[\left(\frac{G_1}{r} + \frac{G_5}{(1-r)}\right) - \sqrt{\left(\frac{G_1}{r} - \frac{G_5}{(1-r)}\right)^2 + \frac{4G_2G_4}{r(1-r)}}\right] \quad \text{(xv)}$$

$$N_1 = -\left[\left(\frac{\frac{G_4}{1-r} + \frac{G_5}{1-r} - A_2}{A_2 - A_1}\right)(T_{F,in} - T_a) + A2A2 - A1G3G4 - G1G6G1G5 - G2G4 + G61 - rA2 - A1\right] \quad \text{(xvi)}$$

$$N_2 = \left(\frac{\frac{G_4}{1-r} + \frac{G_5}{1-r} - A_1}{A_2 - A_1}\right)(T_{F,in} - T_a) + \left(\frac{A_1}{A_2 - A_1}\right)\left(\frac{G_3G_4 - G_1G_6}{G_1G_5 - G_2G_4}\right) + \frac{\frac{G_6}{1-r}}{A_2 - A_1} \quad \text{(xvii)}$$